Biochemical and Functional Characterization of Recombinant *Rhodnius prolixus* Platelet Aggregation Inhibitor 1 as a Novel Lipocalin with High Affinity for Adenosine Diphosphate and Other Adenine Nucleotides

Ivo M. B. Francischetti, John F. Andersen, and José M. C. Ribeiro*

Laboratory of Parasitic Diseases, National Institute of Allergy and Infectious Diseases, 4 Center Drive, Room 4/126, MSC-0425, National Institutes of Health, Bethesda, Maryland 20892-0425

Received May 17, 2001; Revised Manuscript Received September 27, 2001

ABSTRACT: The *Rhodnius prolixus* aggregation inhibitor 1 (RPAI-1) is a novel blood-sucking salivary molecule that binds to ADP and attenuates platelet aggregation. In this report, we determine the binding constants and specificity of RPAI-1 for adenine nucleotides and its functional significance. By the Hummel−Dreyer method of equilibrium gel filtration, we show that RPAI-1 binds ADP with a $K_{0.5}$ of 48.6 ± 12.2 nM. RPAI-1 also displays high-affinity binding to ATP, AMP, Ado, AP4A, and α,*β* Met ADP; however, RPAI-1 does not bind to inosine, guanosine, uridine, or cytidine. Binding is not modified by EDTA, indicating that Ado structure but not phosphate groups or Ca^{2+} is necessary for binding. By computer simulation, we show that RPAI-1 is more effective in scavenging low but not high concentrations of ADP, in contrast to *R. prolixus* apyrase. RPAI-1 inhibits in vitro the ADP-dependent platelet-rich plasma aggregation by collagen (COLL), TRAP, PAF, and A23187 but did not block platelet aggregation by ristocetin or phorbol myristate acetate (PMA) and only slightly attenuated that by convulxin. RPAI-1 prolongs the closure time as assessed with PFA-100, when COLL−Epi but not COLL−ADP cartridges are employed. RPAI-1 also affects platelet-mediated hemostasis time and COLL-induced thrombus formation at high shear as assessed with the Clot Signature Analyzer. We conclude that RPAI-1 exerts an antiplatelet effect due to scavenging of low concentrations of ADP in vitro and in vivo. RPAI-1 is the first lipocalin described so far with unique specificity for adenine nucleotides.

The *Rhodnius prolixus* aggregation inhibitor 1 (RPAI-1)[1] is a 19 kDa protein recently cloned from the salivary gland of the hematophagous kissing-bug *R. prolixus*. RPAI-1 has a unique mechanism of platelet inhibition, because it binds to ADP and blocks ADP-mediated platelet responses (*1*). Accordingly, RPAI-1 inhibits platelet aggregation induced by small doses of most platelet receptor agonists, especially collagen (COLL), thromboxane A2 mimetic (U46619), and arachidonic acid (*1*). Platelet recruitment and full platelet aggregation triggered by these agonists are highly dependent on small doses of secreted ADP (*2*). This new type of platelet aggregation inhibitor may work in concert with other antiplatelet molecules present in the saliva of *R. prolixus*. In fact, an apyrase that destroys ADP has been described in the salivary gland of *R. prolixus* (*3*); in addition, a family of nitric oxide-carrying molecules has been molecularly characterized (*4*). Like RPAI-1, nitrophorins belong to the lipocalin family of proteins (*5*).

The lipocalin superfamily of proteins displays low levels of overall sequence conservation, with the level of sequence identity falling below 20%. However, all lipocalin sequences share sufficient similarity in the form of short characteristic conserved sequence motifs (*5*). In addition, lipocalins are composed of a core set of quite closely related proteins, according to the analysis of lipocalin crystal structures available from plasma retinol-binding protein, *β*-lactoglobulin, and insecticyanin. The large cup-shaped cavity that characterizes the lipocalins is well adapted for ligand binding. The amino acid composition of the pocket, as well as its overall size and conformation, determines specificity (*5*). In fact, a number of distinct ligands have been identified for the lipocalins, including retinol, fatty acids, and pheromones (*5*).

The nucleotide concentration in the blood is under the control of endothelial cell apyrase (CD39), an enzyme that contributes to the antiatherogenic properties of the vessel wall. CD39 exists as a membrane-bound form and a more recently described soluble form (*6*−*9*). Because RPAI-1 also modulates ADP concentration, we attempted to characterize the specificity and the binding constants of RPAI-1 for binding to a number of nucleotides. Since *R. prolixus* salivary glands contain an apyrase in addition to RPAI-1, the role of two inhibitors of ADP-mediated platelet responses coexisting in the same secretion was unclear. Our results show that RPAI-1 is a high-affinity nucleotide-binding lipocalin with a remarkable specificity for molecules possessing adenosine (Ado) in their structure. Although the lipocalin is specific

* To whom correspondence should be addressed. Telephone: (301) 496-3066. Fax: (301) 402-4941. E-mail: jribeiro@nih.gov.

[1] Abbreviations: α,*β* Met ADP, α,*β*-methylene ADP; Ado, adenosine; ADP, adenosine diphosphate; APR4, diadenosine tetraphosphate; AMP, adenosine monophosphate; ATP, adenosine triphosphate; CITF, COLL-induced thrombus formation; COLL, collagen; CI, confidence interval; Cyt, cytidine; EPI, epinephrine; Guo, guanosine; Ino, inosine; K_m, Michaelis−Menten constant; NSAID, nonsteroidal anti-inflammatory drugs; PAF, platelet activating factor; PHT, platelet-mediated hemostasis time; PMA, phorbol myristate acetate; RPAI-1, *R. prolixus* platelet aggregation inhibitor; *RP* apyrase, *R. prolixus* apyrase; SIPA, shear-induced platelet aggregation; TRAP, thrombin receptor activating peptide; Urd, uridine; V_{max}, maximum enzymatic velocity.

10.1021/bi011015s
Published on Web 02/23/2002

for any adenine nucleotide, in vitro and in vivo experiments did provide experimental evidence which leads to the conclusion that the biologic function of RPAI-1 relates to inhibition of ADP-mediated platelet responses. Moreover, data generated by computer simulation indicate that RPAI-1 does not substitute *R. prolixus* apyrase. Due to their kinetic differences, both molecules have distinct, precise, and complementary functions in the prevention of platelet aggregation.

EXPERIMENTAL PROCEDURES

Materials. Ado, AMP, ADP, ATP, diadenosine tetraphosphate (AP4A), α,*β*-methylene ADP (α,*β* Met ADP), Ino, Guo, Urd, Cyd, A23187, PMA, and platelet activating factor (PAF) were obtained from Sigma Chemical Corp. (St. Louis, MO). All other reagents were obtained from Merck Research Laboratories (Darmstadt, Germany) or Sigma.

R. prolixus Aggregation Inhibitor 1 (RPAI-1). RPAI-1 was cloned, expressed, and tested for the inhibition of platelet aggregation as described previously (*1*).

Modified Hummel−Dreyer Method of Equilibrium Gel Filtration. To assess binding of RPAI-1 to nucleotides, 0.76 nmol of RPAI-1 was injected into a Superdex peptide HR/10/30 column (Pharmacia Biotech, Uppsala, Sweden) perfused at 0.5 mL/min with 0.15 M NaCl, 20 mM Tris-HCl (pH 7.3), 0.1 mM $CaCl_2$, 0.1 mM $MgCl_2$, and the indicated concentrations of nucleotides. In some experiments, divalent cations were substituted with 0.1 mM EDTA. The column was equilibrated with at least 5 volumes of the solution before injection of RPAI-1. Because binding of the nucleotide to the lipocalin distorts the absorbance of the complex to a maximum at 260 nm and an isosbestic point at 287 nm, these two wavelengths were used to monitor the column effluent using a model SM4100 dual-wavelength detector from ThermoSeparation Products (Riviera Beach, FL) set at 260 and 287 nm. The serial port output of the detector was monitored and recorded by an in-house program written in Qbasic (Microsoft, Seattle, WA). RPAI-2 eluted as a mix of the monomer and dimer, as reported previously (*1*). Data were analyzed by another in-house program that numerically set to zero both (260 and 287 nm) baseline values anterior to peak elution (to prevent errors due to the uneven zero baseline when computing the ratios), found the monomeric and dimeric peaks, and averaged all ratios for optical density values larger than 50% of the maximal absorbance found at 260 nm. Values found for monomers and dimers were not different; accordingly, both data sets were combined for each experimental point. Because the lipocalin has a much higher molecular mass (MW) than the ligand, and because the molecular sieving column that was used excludes MWs of >20 kDa, we assume that the lipocalin is in equilibrium with the nominal value of the ligand concentration. Three independent column runs were made for each nucleotide concentration that was tested. The increase in the 260 nm/287 nm absorbance ratio following nucleotide binding was modeled with a hyperbolic equation of the type

$$R = R_o + \{[(R_m - R_o)[L]]/(K_{0.5} + [L])\}$$

where R is the observed absorbance ratio, R_o is the absorbance ratio in the absence of a ligand, R_m is the absorbance ratio when the protein is saturated with ligand, $K_{0.5}$ is the ligand concentration at which one-half of the sites are occupied in the protein, and [L] is the molar concentration of the ligand. Typically, seven or eight ligand concentrations were used for each experiment, which were replicated three times, yielding a data set with 21−24 n data points. Accordingly, 1000 nonlinear regressions were performed by random sampling once each of the three replicates for each of the seven or eight ligand concentrations. Reasonable ranges for R_o, R_m, and $K_{0.5}$ were varied (using a Newtonian approach) to obtain the values (within 1% change in the last program iteration) producing the least sum of squares to experimental data points. The combined average and standard deviations for each parameter are thus the bootstrap estimates of the population mean and its standard deviation or standard error (*7*) as reported in Table 1 and elsewhere in the paper.

Table 1: Parameters Deduced from Nonlinear Regression[a]

nucleotide	$K_{0.5}$	R_0[b]	R_{max}[c]
ATP	14.8 ± 7.80	1.49 ± 0.03	2.13 ± 0.08
ADP	48.9 ± 12.20	1.49 ± 0.02	2.24 ± 0.04
AMP	31.8 ± 8.10	1.48 ± 0.02	2.12 ± 0.04
Ado	60.0 ± 6.45	1.46 ± 0.02	2.15 ± 0.01
α,*β* Met ADP	26.9 ± 3.0	1.45 ± 0.02	2.12 ± 0.02
AP4A	18.9 ± 1.6	1.46 ± 0.02	2.38 ± 0.01
ADP (EDTA)	30.9 ± 3.6	1.45 ± 0.02	2.18 ± 0.01

[a] Curve-fitting parameters deduced from nonlinear regression of the changes in the A_{260}/A_{287} absorbance ratios as a hyperbolical function of the indicated nucleotide concentrations. The average and standard errors were obtained by bootstrapping $n - 1$ regressions. [b] Ratio found by nonlinear regression in the absence of nucleotide. [c] Maximum ratio found by nonlinear regression for saturating nucleotide concentrations.

Computer Modeling. Computer modeling was performed using an in-house program with Qbasic software. The activity of apyrases was assumed to follow Michaelian kinetics where

$$v = V_{max}[S]/K_m + [S]$$

The amount of substrate consumed in discrete intervals of 10 ms was computed to generate the curves shown in Figure 4. For potato apyrase, K_m was 100 μM and V_{max} 10 000 μmol of P_i min^{-1} (mg of protein)$^{-1}$ (*8*). For CD39, K_m was 5.9 μM and V_{max} 80 pmol of P_i min^{-1} (mg of protein)$^{-1}$ (*9*). For *R. prolixus* apyrase, K_m was 291 μM and V_{max} 335 μmol of P_i min^{-1} (mg of protein)$^{-1}$ (*3*). In the simulations shown in Figure 4, equal masses per milliliter of enzymes or RPAI-1 were used and equal to 10 μg/mL. No inhibition by the accumulating product was taken into account. The binding of RPAI-1 to ADP was considered complete in less than 10 ms.

Preparation of Platelets and Platelet Aggregation Assays. Platelet-rich plasma was obtained by platelet-pheresis from medication-free platelet donors at the DTM/NIH blood bank under the direction of S. Leitman. Platelets (300 μL) were added to tyrode-BSA in the aggregometer and stirred at 1200 rpm at 37 °C for 1 min before addition of the aggregating agents. In some experiments, RPAI-1 (or tyrode, vehicle) was added at the indicated concentration before addition of the proaggregatory stimulus. Thrombin receptor-activating peptide (TRAP) was diluted in acetic acid (5%), A23187, and PMA in DMSO. PAF was diluted in chloroform and prepared as follows. PAF (26 μL, 1.9 mm) was evaporated under a gentle helium atmosphere. Then 100 μL of PBS (pH 7.4) was added, and the sample (500 μM PAF) was sonicated

at room temperature at a duty cycle of 100% and output control set at 10 (Branson, Danbury, CT). Finally, the sample was diluted to 500 nM in tyrode-BSA [137 mM NaCl, 27 mM KCl, 12 mM $NaHCO_3$, 0.42 mM NaH_2PO_4, 1 mM $MgCl_2$, 5.55 mM glucose, and 0.25% BSA (pH 7.4)]. Convulxin was purified as described previously (*10*).

Whole Blood Aggregometry. Blood was collected in a citric acid/dextrose mixture (ACD), kept at 37 °C in 5% CO_2, and used within 3 h. Aliquots (1 mL) were added to plastic cuvettes, followed by immersion of the impedance electrode. Samples were kept at 37 °C in the aggregometer chamber under agitation for 10 min to stabilize the baseline. RPAI-1 or tyrode (control) was added at the indicated concentrations before addition of COLL.

Platelet Function Analyzer (PFA-100). Through a 21-gauge cannula inserted into an antecubital vein, a 3 mL blood sample was drawn into a monovette containing a buffered citrate solution. An 800 μL sample containing saline or RPAI-1 (3 μM) was placed into the PFA-100 apparatus (Dade International Inc., Miami, FL). The PFA-100 apparatus provides a test cartridge system for in vitro quantitative assessment of platelet function (*11*). The test cartridges simulate an injured blood vessel and are composed of a sample reservoir, a capillary, and a COLL (2 μg)/epinephrine (EPI) (10 μg)- or COLL (2 μg)/ADP (50 μg) (COLL/ADP)-coated membrane with a central aperture. This device uses citrate-anticoagulated venous blood that is forced through a 150 μm aperture in a nitrocellulose membrane, achieving a shear rate of approximately 5000−6000 s^{-1} to attempt to recreate physiological shear rates. The time needed to form a platelet plug occluding the aperture [closure time (CT)] is a measure of the overall function of the platelets. Blood was analyzed within 2 h of collection. To avoid any sampling interference that could affect the interpretation of the results, blood from the same donors was incubated with saline or RPAI-1 and tested as paired for CT using COLL−ADP or COLL−Epi cartridges. The four donors are healthy volunteers working in this department. None of the selected donors have clinical signal or von Willebrand disease or symptoms compatible with primary hemostasis disorders or blood discrasies; they were advised not to take aspirin or other nonsteroidal anti-inflammatory drugs (NSAID) for 2 weeks before the day of the experiment. A minimum of two measurements was performed using the blood from the same donor for each condition (saline vs RPAI-1), using each cartridge (COLL/ADP vs COLL/Epi). Our mean value for COLL−ADP cartridges has been 100.7 ± 4.2 s [91.4−110 s, 95% confidence interval (CI), $n = 14$] and 92 s (71−119 s, 95% CI) for Dade-Behring. Our mean value for COLL−Epi cartridges has been 139.5 ± 5.1 s (128.8−150.2 s, 95% CI, $n = 22$) and 132 s (94−193 s, 95% CI) for Dade-Behring.

Clot Signature Analyzer (CSA). The CSA system provides an in vitro blood flow pathway environment for simultaneously assessing platelet aggregation and blood coagulation. The functioning of CSA has been described in detail by Li et al. (*12*); collection of blood and handling of the CSA device were performed exactly as described in the User's Manual (Xylum Co.), under the direction of M. Horne III (Department of Clinical Pathology, National Institutes of Health). Briefly, blood (3 mL) was collected using prewarmed (37 °C) 3 cm^3 slip-tip syringes (Becton-Dickson, Rutherford, NJ) containing saline (control, for cartridge 1) or RPAI-1 (3 μM, for cartridge 2) and then appropriately placed in the CSA for estimation of platelet hemostasis time (PHT) and clotting time (CT). Experiments were initiated automatically using software provided by the manufacturer. When the first experiment was completed 30 min latter, blood was drawn again from the same donor as described above and two other cartridges (control vs RPAI-1) were placed in the CSA for estimation of the extent of collagen-induced thrombus formation (CITF).

The CSA has two channels. In the punch channel, the CSA stimulates vascular injury by piercing the blood lumen with a 0.015 cm needle, forming two small holes. Blood flow is partially diverted out through these punch holes. Thus, at the punch hole, the rate of luminal flow decreases significantly, causing the pressure in the pressure chamber to drop from its initial stabilized value of ∼60 mmHg to ∼10 mmHg. In approximately 5 min, blood will cause closure of the two punch holes. At hole closure, luminal blood flow is restored and the pressure chamber pressure recovers to its initial stabilization value. This step is known as the PHT. The blood flowing in the lumen eventually coagulates, forming a clot and causing cessation of luminal flow (CT). Our mean value for PHT is 4:58 ± 0:33 min (2:45−6:50 min, 95% CI), and it is 3:55 min (1:42−6:18 min, 95% CI) as obtained by Xylum Co. Our mean value for CT is 24:01 ± 2:02 min (17:50−30:43 min, 95% CI), and it is 18:20 min (17:54−29:06 min, 95% CI) as obtained by Xylum Co. The collagen channel is a separate flow path similar to but distinct from the punch channel. In the collagen channel, a 1.9 cm collagen fiber is immobilized in the lumen and aligned with the direction of flow. This substrate simulates the exposed subendothelial tissue in vascular biology. As blood flows, the platelet adheres to the collagen, initiating thrombus formation, the step known as CITF. Our mean value for CITF is 5:04 ± 1:02 min (2:56−7:52 min, 95% CI), and it is 5:58 min (4:24−8:12 min, 95% CI) as obtained by Xylum Co.

Statistical Analysis. For PFA-100, statistical comparisons were paired analyses between the means. Because a normality of distribution could not be assured (*11*), nonparametric analysis was performed with the Wilcoxon paired test using GraphPad Prism (GraphPad Software Inc., New York, NY). For experiments with CSA, significance was calculated using the Student's *t* test for paired data (two-tailed), assuming a parametric distribution (*12*). Significance was set at $p \leq 0.05$.

RESULTS AND DISCUSSION

We have previously shown that RPAI-1 inhibits ADP-mediated platelet responses through binding to the nucleotide. In fact, the spectrum of RPAI-1 in the presence of ADP is remarkably modified at 260 nm, a pattern of spectral change that is consistent with a molecule that binds ADP (*13*). In this report, a protocol has been optimized in an attempt to characterize the dissociation constant for dissociation of ADP from RPAI-1 and identify additional ligands for this lipocalin. This protocol is based on a technique known as the Hummel−Dreyer method of equilibrium gel filtration (*14*). This gel filtration method is useful in the detection and characterization of interactions between two proteins when the complex they form is dynamic and equilibrates on a time scale faster than or comparable to the running time. It is also useful to determine the dissociation constant between two ligands (*14*).

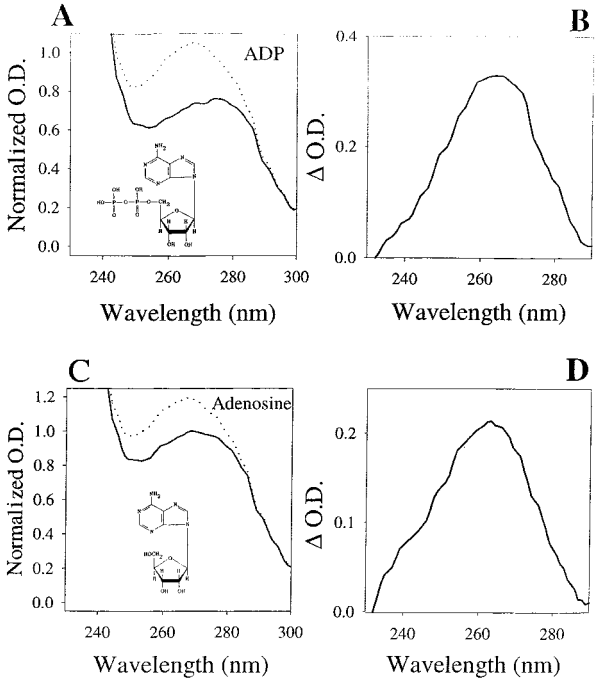

FIGURE 1: High-affinity binding of Ado and ADP to RPAI-1. Spectrum of RPAI-1 as it elutes from a molecular sieving column in the absence (—) and in the presence (···) of (A) 1 μM ADP, with the differential spectrum in panel B, and (C) 1 μM Ado, with the differential spectrum in panel D. The insets show the chemical formulas for these compounds.

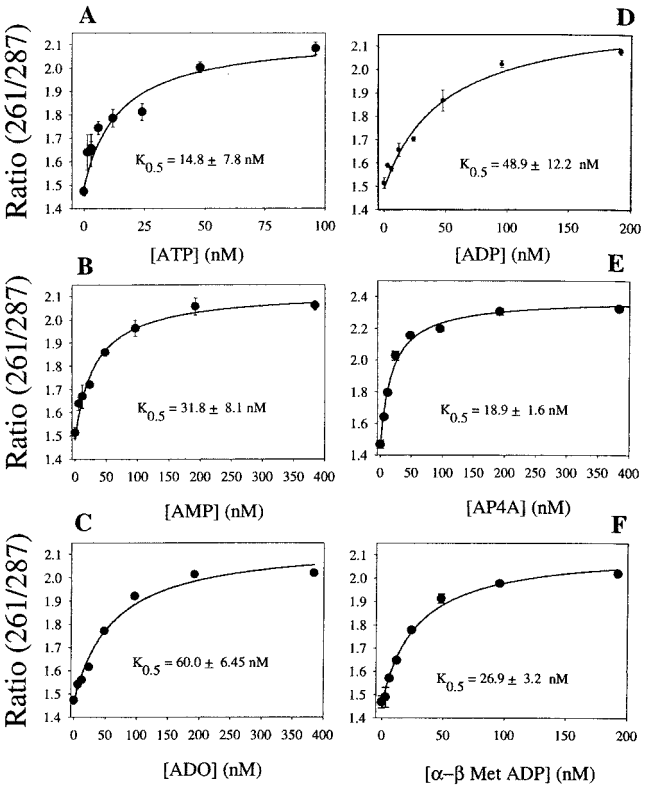

FIGURE 2: Saturation curves representing binding of Ado and Ado nucleotides to RPAI-1. Ratios of the absorbance measured at 261 and 287 nm at different concentrations of adenine nucleotides. The symbols and bars represent the average and standard errors, respectively, of three independent measurements. The fitted curve was obtained by bootstrap of 23 nonlinear regressions performed on the data set. All experiments were carried out in the presence of 0.1 mM $CaCl_2$ and 0.1 mM $MgCl_2$.

Figure 1A depicts a typical profile of the RPAI-1 spectrum between 230 and 300 nm in the absence of ADP (solid lines). The column was then equilibrated with ADP, followed by addition of RPAI-1 previously incubated with the same concentrations of ADP. Elution of the ADP−RPAI-1 complex was achieved with an elution buffer also containing equivalent concentrations of ADP for each data point. In the presence of ADP (1 μM), an increase in RPAI-1 absorbance at 260 nm is observed (dotted lines). Figure 1B shows the differential spectrum of RPAI-1 obtained with and without ADP. We next tested the hypothesis that negatively charged groups linked to Ado would be preferential ligands for RPAI-1. This assumption was based on the crystal structure of kinesine with ADP, where formation of a stable complex has been reported to be dependent on the negatively charged phosphates present in the ADP (and AMP) molecules (*15*). In addition, RPAI-1 is highly basic, with a predicted pI of 10.1 (*1*), suggesting that it could preferentially bind anionic ligands; however, RPAI-1 also binds Ado, an adenine nucleotide containing no phosphate groups (Figure 1C). The differential spectrum is shown in Figure 1D.

When the A_{260}/A_{287} ratios of n independent experiments are fit by simple hyperbolic equations by nonlinear regression methods, a good fit of the data is obtained (Figure 2A−F). Accordingly, binding is specific, and saturation is reached at ~200 nM nucleotides with a half-maximum saturation ($K_{0.5}$) of ~15−60 nM. These data indicate that the binding of ADP to RPAI-1 is high affinity binding and follows a simple hyperbolic saturation curve. Accordingly, RPAI-1 binds to ATP with a $K_{0.5}$ of 14.8 ± 7.8 nM (Figure 2A), AMP with a $K_{0.5}$ of 31.8 ± 8.1 nM (Figure 2B), Ado with a $K_{0.5}$ of 60.0 ± 6.45 nM (Figure 2C), and ADP with a $K_{0.5}$ of 48.6 ± 12.2 nM (Figure 2D). Binding of RPAI-1 to ADP is independent of divalent ion, because EDTA (0.1 mM) did not significantly change the $K_{0.5}$ of RPAI-1 for ADP ($K_{0.5}$ = 30.9 ± 3.6 nM) (not shown). Figure 2 also shows that RPAI-1 binds additional molecules containing Ado and possessing biologic activity, such as AP4A with a $K_{0.5}$ of 18.9 ± 1.6 nM (Figure 2E) and the nonhydrolyzable ADP analogue α,β Met ADP with a $K_{0.5}$ of 26.9 ± 3.2 nM (Figure 2F).

To study the structural requirements for binding, additional Ado nucleotides were tested. RPAI-1 only slightly interacts with Guo, Urd, and Cyt at 1 μM (Figure 3A−C), and no interaction was observed with Ino, the product of Ado deamination (Figure 3D). Together, these data indicate that the interaction of RPAI-1 with ADP and other Ado-related compounds is not dependent on the phosphate groups but rather is dependent on the Ado structure. In particular, the NH_2 group must be important, indicated by the lack of Ino binding to RPAI-1 or by Guo, which has an oxygen instead of the amino group. Table 1 summarizes the binding constants obtained for each RPAI-1 nucleotide interaction.

Because a typical apyrase has been kinetically characterized in the salivary gland of *R. prolixus* (*3*) [*R. prolixus* apyrase (*RP* apyrase)], the biologic significance of the coexistence of two nucleotide binding proteins in the same secretion turned out to be uncertain. In an attempt to answer this question, computer simulations were employed where the time (in seconds) was used as an estimate to compare the efficiencies of enzymes and RPAI-1 according to their

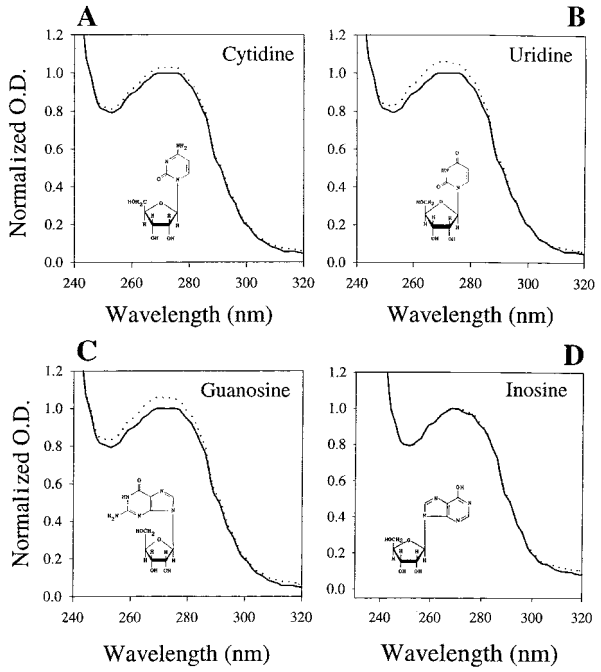

FIGURE 3: RPAI-1 does not bind to Guo, Urd, Cyt, or Ino. RPAI-1 as it elutes from a molecular sieving column in the absence (—) and in the presence (···) of 1 μM Cyt (A), Urd (B), Guo (C), or Ino (D). The insets show the chemical formulas for these compounds.

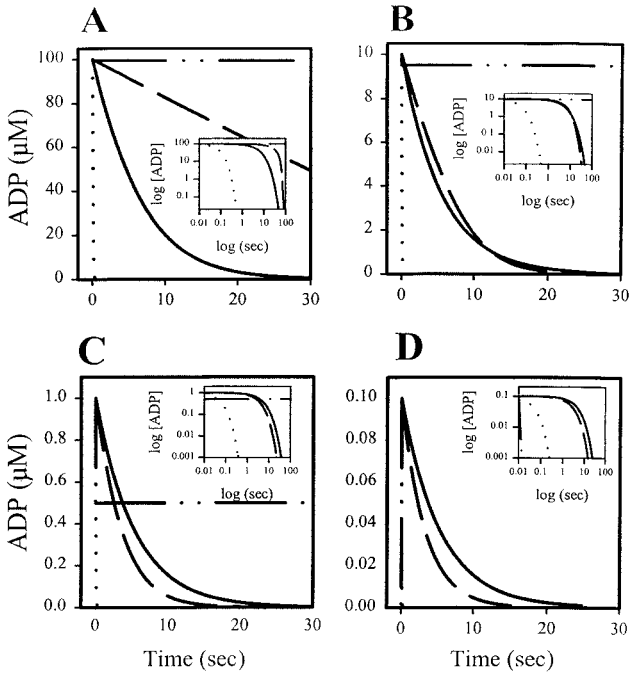

FIGURE 4: Computer simulation of the degradation of ADP by different nucleotide-binding proteins. The time in seconds necessary for hydrolyzing/scavenging of the ADP concentration by RPAI-1 (—••—), CD39 (— — —), *RP* apyrase (—), and potato apyrase (···) estimated assuming a Michaelis−Menten equation where $v = V_{max}[S]/K_m + [S]$. ADP concentrations were (A) 100, (B) 10, (C) 1, and (D) 0.1 μM. The insets show plots of log ADP concentration vs log time in seconds. All enzymes and RPAI-1 were simulated to be at a concentration of 10 μg/mL.

K_m and V_{max} values, or binding ability of RPAI-1 according to its $K_{0.5}$. Figure 4A shows that using either 10 μg/mL enzyme or RPAI-1 (—••—), and at high ADP concentrations (100 μM), only potato apyrase (···), an enzyme with low affinity (K_m = 100 μM) but extremely high V_{max} (10 000 μmol of P_i mol^{-1} mg^{-1}), rapidly destroys ADP, followed by *RP* apyrase [K_m = 290 μM; V_{max} = 300 μmol of P_i min^{-1} (mg of protein)$^{-1}$] depicted as continuous lines and CD39 [K_m = 5.9 μM; V_{max} = 72 pmol of P_i min^{-1} (mg of protein)$^{-1}$] shown as dashed lines. Accordingly, more than 20 s elapse before CD39 and *RP* apyrase can decrease ADP concentrations to <0.1 μM. As expected, the ADP concentration was almost not affected by RPAI-1.

At moderate concentrations of ADP (10 μM), CD39 is as effective as *RP* apyrase; RPAI-1 slightly affects ADP concentration, and potato apyrase rapidly destroys the nucleotide. Still, CD39 and *RP* apyrase take more than 10 ms to lower the ADP concentration to <0.1 μM. At low concentrations of ADP (1 μM), RPAI-1 instantaneously scavenges 50% of the ADP concentration; as expected, *RP* apyrase and CD39 are less effective. The effect of RPAI-1 is remarkable at 0.1 μM ADP, where it immediately brings the ADP concentration to sub-nanomolar levels. In contrast, it takes ~0.3 s for potato apyrase to destroy ADP, whereas it takes ~20 and 40 s for CD39 and *RP* apyrase, respectively, to remove ADP (see the figure insets). These findings are also thermodynamically supported by the Haldane equation, which states that an increase in substrate affinity cannot be accompanied by an increase in the rate of enzyme turnover, unless the affinity for products is decreased in a higher proportion (*16*).

The simulation results shown in Figure 4 indicate that a high-affinity nucleotide-binding protein (RPAI-1) is functionally more effective in removing very low concentrations of ADP. In contrast, *RP* apyrase the antiaggregatory function is less remarkable at low concentrations of ADP, at the expenses of its high K_m for ADP. In fact, effective destruction of ADP by the *RP* apyrase occurs when the ADP concentration is at least 1000−5000-fold higher (50 μM) than that readily removed by RPAI-1 (Figure 4A,B). In this context, it should be emphasized that the ADP physiologic plasmatic concentration is ~0.1 μM (*17*), and it can reach 1−2 μM at the site of injury provoked by a Simplate device (*18*); 0.2−0.4 μM ADP is known to be biologically active (*19*−*22*). We conclude that RPAI-1 and *RP* apyrase coexisting in the same secretion have precise and complementary biologic functions in the prevention of platelet aggregation.

RPAI-1, accordingly, should prevent platelet aggregation in those circumstances where low concentrations of ADP are known to be important for agonist action, such as small doses of collagen (COLL), arachidonic acid (AA), thromboxane A2 mimetics (U46069), and platelet-activating factor (PAF), but not important for phorbol myristate acetate (PMA), ristocetin, or convulxin-induced platelet aggregation. Indeed, RPAI-1 does inhibit ADP-dependent platelet-rich plasma aggregation triggered by low concentrations of COLL (Figure 5A), AA (Figure 5B), and U46069 (Figure 5C), confirming previous results obtained when a microplate reading was used to assess platelet function (*1*). We show additionally that RPAI-1 also inhibits platelet aggregation triggered by TRAP (Figure 5D), PAF (Figure 5E), and ionophore A23187 (Figure 5F) at concentrations mediated by ADP (*23*−*25*). On the other hand, it does not affect platelet aggregation triggered by ristocetin (Figure 5G) or PMA (Figure 5H) (*26*, *27*), or only slightly affected by small doses of convulxin (Figure 5I) (*1*, *28*). The in vitro inhibition

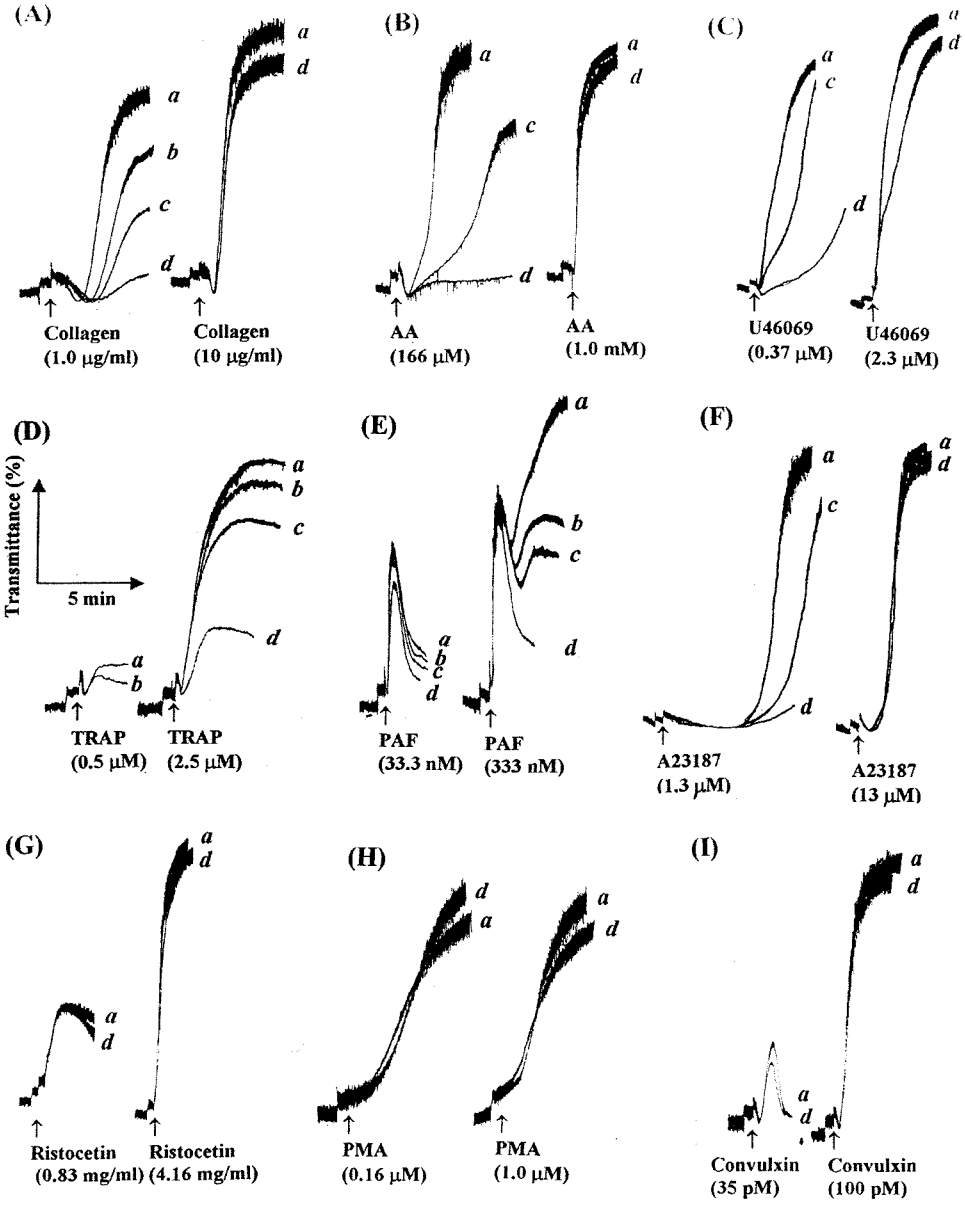

FIGURE 5: In vitro inhibition of platelet-rich plasma aggregation by RPAI-1. Platelets were incubated with (a) 0, (b) 0.33, (c) 1, and (d) 3 μM RPAI-1 followed by addition of (A) COLL, (B) arachidonic acid (AA), (C) U46069 (TXA2 mimetic), (D) PAF, (E) TRAP, (F) A23187 (Ca^{2+} ionophore), (G) ristocetin, (H) PMA, and (I) convulxin. Ligand concentrations are indicated. Typical tracings are depicted.

of platelet aggregation by RPAI-1 depicted in Figure 5 is also consistent with the low concentration of ADP reached in the aggregation cuvette upon stimulation (*19*−*22*) that is above the calculated $K_{0.5}$ of RPAI-1 for ADP (Table 1). Finally, the actions of RPAI-1 should not be restricted to the agonists employed in Figure 5; platelet aggregation by cathepsin G (*29*), plasmin (*30*), chemokines (*31*), and FcγRIIA cross-linking (*32*) is also dependent on ADP. We could also demonstrate that small (2 μg/mL) doses of COLL induced whole blood platelet aggregation, as detected by an increase in impedance, which was dose-dependently inhibited by RPAI-1. As expected, this effect was not observed at high concentrations (15 μg/mL) of COLL (not shown). Taken together, the data shown in Figure 5 indicate that other adenine nucleotides or Ado in plasma is not at a concentration sufficiently high to outcompete ADP binding to RPAI-1.

Because it is well-known that blood-sucking insects feed on small arterioles, although not exclusively (*33*), it was of interest to establish whether RPAI-1 could affect platelet aggregation under high shear. In fact, besides activation by a thrombogenic surface (e.g., COLL), platelets are exposed to shear forces that are produced by different velocities of blood flowing near the vessel wall; shear forces are greater in arteries than in veins, and particularly in small arterioles and capillaries and in partially obstructed vessel lumen (*34*, *35*). Shear-induced platelet aggregation (SIPA) occurs by a mechanism dependent on the von Willebrand factor, glycoprotein (GP) Ibα, integrin αIIbβ3, and ADP, but it is not affected by aspirin or indomethacin (*36*, *37*).

To test the effects of RPAI-1 under shear conditions, we have used a Platelet Function Analyzer (PFA-100) where citrated blood is forced to pass through an aperture containing COLL−ADP or COLL−Epi cartridges at high shear (6000 s^{-1}) and the time for closure is indicative of platelet function (*11*). Figure 6 shows that when COLL−ADP cartridges are used with control blood (no inhibitor), the aperture occludes

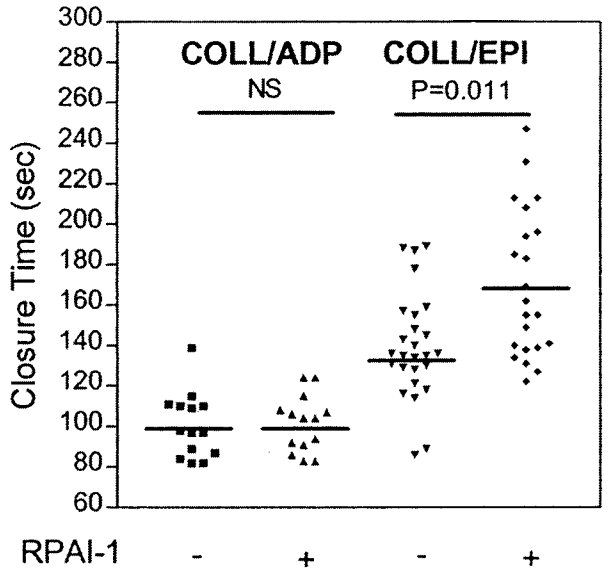

FIGURE 6: Scatter graph of closure times obtained using PFA-100. RPAI-1 (3 μM) prolongs COLL−Epi ($p = 0.011$, $n = 22$), but not COLL−ADP ($p = 0.5$, $n = 14$, NS) cartridge closure time (seconds). NS means nonsignificant.

in 100.7 ± 4.2 s (91.4−110 s, 95% CI); in the presence of RPAI-1, the closure time is almost identical [101.5 ± 3.6 s (93.52−109.5 s, 95% CI)]. It is plausible to suggest that the amount of ADP released by COLL−ADP cartridges surmounts the binding capacity of RPAI-1, or alternatively, the high concentration of ADP immobilized in the cartridge substitutes released ADP as a proaggregatory stimulus. When COLL−Epi cartridges were used, the CT was significantly ($p = 0.011$) increased in the presence of RPAI-1. The control CT has been 139.5 ± 5.1 s (128.8−150.2 s, 95% CI) and 169.63 ± 7.7 s (153.4−185.9 s, 95% CI) in the presence of RPAI-1 (Figure 6). It is conceivable to conclude that when COLL−Epi cartridges are employed the amount of ADP released is smaller than that with COLL−ADP cartridges, and this amount is effectively scavenged by RPAI-1, resulting in a prolonged CT. This assumption is consistent with the identification of ADP as a key molecule that provides additional signaling for full platelet aggregation through binding to a recently characterized receptor that couples to adenyl cyclase (*38*). Interestingly, the effects of RPAI-1 and aspirin are similar in this respect since both inhibitors increase the CT only when COLL−Epi cartridges are employed. In the case of aspirin, however, this is due to blockade of ADP release by cyclooxygenase inhibitors (*39*), whereas for RPAI-1, this must be due to scavenging of released ADP. Finally, the finding that RPAI-1 affects the CT uniquely when the COLL−Epi cartridges are used indicates that variation in collagen receptor density does not play a major role in the results described in Figure 6. In fact, it has been shown that low levels or polymorphism of $\alpha_2\beta_1$ dictate the level of platelet adhesion to collagen in the general population (*41*), or correlate with impaired platelet function in a high-shear stress system, in von Willebrand disease patients (*42*).

In an attempt to provide additional data to support the contention that RPAI-1 affects shear-induced platelet aggregation, we used a Clot Signature Analyzer (*12*). This device detects platelet function at high shear rates encountered in small arteries; it uses noncoagulated blood and

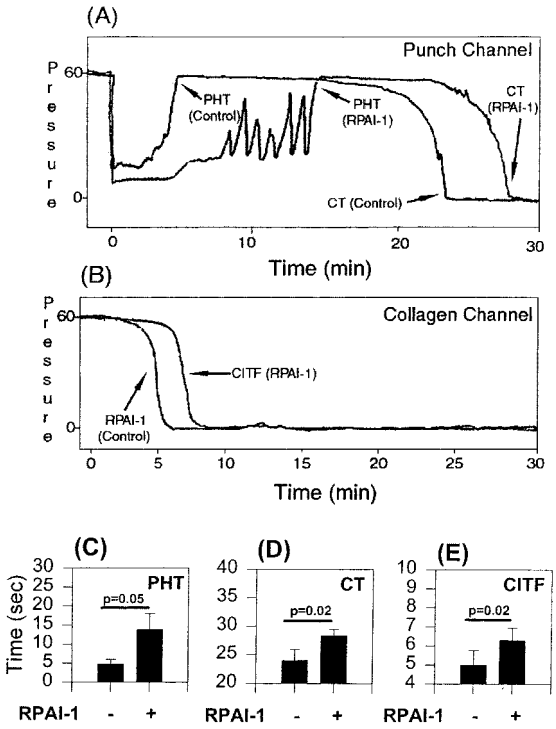

FIGURE 7: RPAI-1 inhibits COLL-induced platelet responses in whole blood and high shear. Typical experiments depict the effects of RPAI-1 on (A) platelet hemostasis time (PHT) and clotting time (CT) and (B) COLL-induced thrombus formation (CITF). The measurements were initiated at time zero minutes. Pressure is given in millimeters of Hg. The effects of RPAI-1 on (C) PHT, (D) CT, and (E) CITF are shown as the means ± SE of four independent experiments.

contains two channels. In the punch channel, thrombogenic material is not present; in contrast to PFA, bleed arrest occurs exclusively by a shear-mediated process, resembling the O'Brien filter for studying SIPA (*43*). A plastic tube is rapidly punched transversally with a needle, with a decrease in pressure due to the loss of blood through the two orifices that have been created. At high shear, two platelet plugs will eventually become strong enough to seal the injury sites and allow blood to continue to flow in the pathway. At this point, the pressure will recover and be reported quantitatively as the PHT. Figure 7A shows a typical tracing depicting that PHT was remarkably affected by RPAI-1. Our mean value for PHT has been 4:58 ± 0:33 min (2:45−6:50 min, 95% CI) in control samples and 14:18 ± 3:48 min (6:46−20:50 min, 95% CI) in the presence of RPAI-1 ($p = 0.05$) (Figure 7C), suggesting that inhibition of ADP-mediated stable platelet aggregation is accompanied by the development of an unstable hemostatic plug indicated by the tracing oscillation in Figure 7A. In fact, it has been shown that ADP is involved in irreversible platelet aggregation by a PI-3-kinase-dependent pathway (*32*). After pressure recovery (plug formation), blood coagulation takes place; the time it takes for the blood to clot and stop blood flow (drop of pressure) is taken as the CT. Figure 7A also shows that the CT was prolonged by RPAI-1. For these experiments, the average CT has been 24:01 ± 2:02 min for control samples (17:50−30:43 min, 95% CI) and 28:39 ± 1:11 min for RPAI-1-treated samples (24:55−31:40 min, 95% CI) ($p = 0.02$) (Figure 7D). The COLL channel can be used to assess the adhesion and aggregation of platelets to COLL under high

shear, and the time necessary for the thrombus to occlude the vessel is taken as the CITF. Figure 7B depicts a typical result out of four independent experiments performed with CSA, showing an increase in the level of CITF in the presence of RPAI-1. The average control sample for CITF occurs in 5:04 ± 0:55 min (2:56−7:52 min, 95% CI); in contrast, it takes 6:29 ± 0:58 min (4:14−8:44 min, 95% CI) in the presence of RPAI-1 ($p = 0.02$) (Figure 7E). This suggests that ADP released by adherent platelets contributes to thrombus formation at high shear by inducing platelet recruitment and activation of integrin $\alpha_{IIb}\beta_3$ that serves as a binding site for vWf (*34*−*37*).

Taken together, these data provide strong experimental evidence that RPAI-1, which coexists with *RP* apyrase, most likely behaves in vivo and in vitro as an efficient ADP scavenger at low nucleotide concentrations. Together with endothelial cell apyrase (CD39) and soluble CD39, RPAI-1 may modulate the ADP concentration at the site of vascular injury (*44*). RPAI-1 removes free ADP from plasma without producing AMP or Ado, which are products by apyrases and 5′-nucleotidases. Because AMP and Ado affects platelet aggregation (*45*), RPAI-1 is a unique reagent for studying the role of ADP in platelet function, without confounding effects of its breakdown products. Additionally, because ADP has been involved in thrombus formation (*22*), xenographic rejection (*46*), and microaggregate formation in extracorporeal circulation (*47*), we speculate that these conditions may be attenuated by RPAI-1. RPAI-1 is the first component of the lipocalin superfamily of proteins (*48*) that has been characterized so far with specificity for adenine nucleotides.

ACKNOWLEDGMENT

We are grateful to Drs. Robert Gwadz, Thomas Kindt, and Louis H. Miller for encouragement and support. We are thankful to Drs. S. Leitman and C. Matthews at the Department of Transfusional Medicine at the NIH Clinical Center for providing fresh platelet-rich plasma. We thank Dr. McDonald Horne III, Ms. S. Williams, and K. Ngyen of the Hematology Section (Department of Clinical Pathology, NIH Clinical Center) for helping with the PFA-100 and CSA experiments. We also thank Brenda Rae Marshall for editorial revision of the manuscript.

REFERENCES

1. Francischetti, I. M. B., Ribeiro, J. M. C., Champagne, D., and Andersen, J. (2000) *J. Biol. Chem. 275*, 12639−12650.
2. Paul, B. Z. S., Jin, J., and Kunapuli, S. P. (1999) *J. Biol. Chem. 41*, 29108−29114.
3. Sarkis, J. J. F., Guimarães, J. A., and Ribeiro, J. M. C. (1986) *Biochem. J. 233*, 885−891.
4. Ribeiro, J. M., Hazzard, J. M., Nussenzveig, R. H., Champagne, D. E., and Walker, F. A. (1993) *Science 23*, 539−541.
5. Flower, D. R. (1996) *Biochem. J. 318*, 1−14.
6. Kaczmarek, E., Koziak, K., Sevigny, J., Siegel, J. B., Anrather, J., Beaudoin, A. R., Bach, F. H., and Robson, S. C. (1996) *J. Biol. Chem. 271*, 33116−33122.
7. Efron, B., and Tibshirani, R. (1991) *Science 253*, 390−395.
8. Handa, M., and Guidotti, G. (1996) *Biochem. Biophys. Res. Commun. 218*, 916−923.
9. Gayle, R. B., III, Maliszewski, C. R., Gimpel, S. D., Schoenborn, M. A., Caspary, R. G., Richards, C., Brasel, K., Price, V., Drosopoulos, J. H. F., Islam, N., Alyonycheva, T. N., Broekman, M. J., and Marcus, A. J. (1998) *J. Clin. Invest. 101*, 1851−1859
10. Francischetti, I. M., Saliou, B., Leduc, M., Carlini, C. R., Hatmi, M., Randon, J., Faili, A., and Bon, C. (1997) *Toxicon 35*, 1217−1228.
11. Mamme, E. F., Comp, P. C., Gosselin, R., Greenberg, C., Hoots, W. K., Kessler, C. M., Larkin, E. C., Liles, D., and Nugent, D. J. (1998) *Semin. Thromb. Hemostasis 24*, 195−202.
12. Li, C. K., Hoffman, T. J., Hsied, P. Y., Malik, S., and Watson, W. C. (1998) *Thromb. Res. 92*, S67−S77.
13. Bock, R. M., and Ling, N. S. (1956) *Arch. Biochem. Biophys. 62*, 253−258.
14. Beeckmans, S. (1999) *Methods 19*, 278−305.
15. Muller, J., Marx, A., Sack, S., Song, Y.-H., and Mandelkow, E. (1999) *Biol. Chem. Hoppe-Seyler 380*, 981−992.
16. Mahler, H. R., and Cordes, E. H. (1971) in *Biological Chemistry, Enzyme Kinetics*, Chapter 6, pp 267−324, Harper & Row Publishers, New York.
17. Enjyoji, K., Sevigny, J., Lin, Y., Frernette, P. S., Christie, P. D., Esch, J. S., II, Imai, M., Edelberg, J. M., Rayburn, H., Lech, M., Beeler, D. L., Csizmadia, E., Wagner, D. D., Robson, S. C., and Rosenberg, R. D. (1999) *Nat. Med. 5*, 1010−1017.
18. Born, G. V. R., and Kratzer, M. A. A. (1984) *J. Physiol. 354*, 419−429.
19. Cattaneo, M., Lombardi, R., Zighetti, M. L., Gachet, C., Ohlmann, P., Cazenave, J.-P., and Mannucci, P. M. (1997) *Thromb. Haemostasis 77*, 980−990.
20. Jin, J., and Kunapuli, S. P. (1998) *Proc. Natl. Acad. Sci. U.S.A. 95*, 8070−8074.
21. Selheim, F., Froyset, A. K., Strand, I., Vassbotn, F. S., and Holmsen, H. (2000) *FEBS Lett. 485*, 62−66.
22. Marcus, A. J., and Safier, L. B. (1993) *FASEB J. 7*, 516−522.
23. Rao, A. K., Willis, J., Hassell, B., Dangelmaier, C., Holmsen, H., and Smith, J. B. (1984) *Am. J. Hematol. 17*, 153−165.
24. Penny, W. F., and Ware, J. A. (1992) *Blood 79*, 91−98.
25. Rittenhouse, S. E. (1984) *Biochem. J. 222*, 103−110.
26. Rick, M. E. (1994) *Clin. Lab. Med. 14*, 781−794.
27. Watson, S. P., McNally, J., Shipman, L. J., and Godfrey, P. P. (1988) *Biochem. J. 249*, 345−350.
28. Francischetti, I. M. B., Ghazaleh, F. A., Reis, R. A. M., Carlini, C. R., and Guimarães, J. A (1998) *Arch. Biochem. Biophys. 353*, 239−250.
29. Kinlough-Rathbone, R. L., Perry, D. W., Rand, M. L., and Pakham, M. A. (1999) *Thromb. Res. 95*, 341−346.
30. Ishii-Watabe, A., Uchida, E., Mizuguchi, H., and Hayakawa, T. (2000) *Biochem. Pharmacol. 59*, 1345−1355.
31. Gear, A. R., Suttitanamongkol, S., Viisoreanu, D., Polanowska-Grabowska, R. K., Raha, S., and Camerini, D. (2001) *Blood 97*, 937−945.
32. Gratacap, M. P., Herault, J. P., Viala, C., Ragab, A., Savi, P., Herbert, J. M., Chap, H., and Payrastre, B. (2000) *Blood 96*, 3439−3446.
33. Gordon, R. M., and Crewe, W. (1948) *Ann. Trop. Med. Parasitol. 42*, 334−356.
34. Ruggeri, Z. M. (1993) *Thromb. Haemostasis 70*, 119−123.
35. Ikeda, Y., Handa, M., Kawano, K., Kamata, T., Murata, M., Araki, Y., Anbo, H., Kawai, Y., Watanabe, K., Itagaki, I., Sakai, K., and Ruggeri, Z. M. (1991) *J. Clin. Invest. 87*, 1234−1240.
36. Moake, J. L., Turner, N. A., Stathopoulos, N. A., Nolasco, L. H., and Hellums, J. D. (1988) *Blood 71*, 1366−1374.
37. Cattaneo, M., Lombardi, R., Bettega, D., Lecchi, A., and Mannucci, P. M. (1993) *Arterioscler. Thromb. 13*, 393−397.
38. Hopppeter, G., Jantzen, H. M., Vincent, D., Li, G., England, L., Ramkrishnan, V., Yang, R. B., Nurden, P., Nurden, A., Julius, D., and Conley, P. B. (2001) *Nature 409*, 202−207.
39. Gaziano, J. M., Skerrett, P. J., and Buring, J. E. (2000) *Haemostasis 30*, 1−13.
40. Mammen, E. F., Alshameeri, R. S., and Comp, P. C. (1995) *Semin. Thromb. Hemostasis 21*, 113−121.
41. Kunicki, T. J., Orchekowski, R., Annis, D., and Honda, Y. (1993) *Blood 82*, 2693−703.

42. Di Paola, J., Federici, A. B., Mannucci, P. M., Canciani, M. T., Kritik, M., Kunicki, T. J., and Nurgent, D. (1999) *Blood 93*, 3578−3582.
43. O'Brien, J. R., and Salmon, G. P. (1987) *Blood 70*, 1354−1361.
44. Qawi, I., and Robson, S. C. (2001) *Curr. Drug Targets 2*, 213−214.
45. Bullogh, D. A., Zhang, C., Montag, A., Mullane, K. M., and Young, M. A. (1994) *J. Clin. Invest. 94*, 1524−1533.
46. Imai, M., Takigami, K., Guckelberger, O., Enjyoji, K., Smith, R. N., Csizmadia, E., Sevigny, J., Rosenberg, R. D., Bach, F. H., and Robson, S. C. (1999) *Mol. Med. 5*, 743−752.
47. Hall, M. W., Goodman, P. D., Solen, K. A., and Mohammad, S. F. (2000) *ASAIO J. 46*, 693−695.
48. Flower, D. R. (2000) *Biochim. Biophys. Acta 1482*, 327−336.

BI011015S